International Journal of Research
Available at https://edupediapublications.org/journals
p-ISSN: 2348-6848
e-ISSN: 2348-795X
Volume 03 Issue 18
December 2016

Renewable energy system Based Stand-Alone system for DC-AC Converter fed BLDC Motor

Guggilla.sirisha,
M-tech Student Scholar,
Department of Electrical & Electronics Engineering,(PE&D)
M.V.R college of Engineering& Technology, Paritala ,Krishna (Dt),A.P,India.
Email:guggillasirisha244@gmail.com

MD. Kouser,
Assistant Professor,
Department of Electrical & Electronics Engineering,
M.V.R college of Engineering &Technology,Paritala,
Krishna (Dt); A.P, India.
Email:mohamadkouser4@gmail.com

Rushi Santhosh Singh Thakur,
Associate Professor,
HOD,Department of Electrical & Electronics Engineering,
M.V.R College of Engineering&Technology, Paritala,
Krishna (Dt), A.P, India.
Email:rushib4u@gmail.com

Abstract-This paper proposes an effective Maximum Power Point Tracking (MPPT) controller being incorporated into a solar Photovoltaic system supplying a Brushless DC (BLDC) motor drive as the load. With solar customers in many states now receiving a low price for electricity sold back to the grid, battery back-up systems can be available alternative as they use the electricity stored during the day to run your house at night. In order to address this issue, a two-stage stand-alone scheme consisting of a novel transformer coupled dual-input converter (TCDIC) followed by a conventional full-bridge inverter is proposed. The proposed TCDIC can realize maximum power point tracking and battery charge control while maintaining the proper voltage level at the load terminal. A suitable control strategy for the proposed TCDIC devised for manipulating the TCDIC to realize the first two aforementioned objectives, while the third objective is achieved by employing a conventional proportional integral (PI) controller to control the output voltage of the full bridge inverter through sinusoidal pulse width modulation. Due to significant increase in the demand of electric motors, design and manufacturing of high efficiency motors and related variable speed drives has been a major interest by many suppliers. Brushless DC (BLDC) motor has many advantages including high torque capability. The simulation results are performed by using Matlab/Simulink software.

Index Terms—Battery charge control, dual-input dc–dc converter, PV-based stand-alone scheme, solar photovoltaic (PV) converter, BLDC Motor.

I.INTRODUCTION

Nowadays, we face exponentially increasing demand of energy which inadvertently requires the use of non-renewable sources such as coal and natural gas. Since these sources are constrained, they have a tendency to become depleted and also contribute to environmental pollution to a large extent. Apart from the fundamental limitations of fossil fuel, ecological considerations in the manner of the greenhouse gases and global warming are the variant prominent forces associated with the promotion of renewable energy sources. Hence, the evident choice of a renewable energy source is one that is found in abundance, and provides security for future enlargement and growth. It is the energy harnessed from the sun. The sun is an enormous energy source. The earth receives an average of 1.8 × 1011 MW power from the sun which is infinitely larger than that consumed from the rest of the sources of energy combined [1-3].

Abundance of solar energy makes it the most sought after energy source that can be easily converted into electrical energy using Photovoltaic (PV) arrays. Standalone applications of PV energy are quite prevalent. Applications such as water pumping, household appliances, fans, electrification of rural areas where the availability of grid connection, air conditioning, etc. is yet to be implemented using PV electricity. In spite of several advantages like superior dynamic response, increased efficiency, ease of maintenance, better speed-torque characteristics and long operating life, it seems that less ample attention has been given to the feasibility of using PV systems to actuate Brushless DC (BLDC) motors. The performance of DC motors and AC induction type motors energized by PV sources has been analysed in the literature [4-7]. In this proposed method, the usage of BLDC motor yields the highest efficiency in comparison with all conventional motors, and also demonstrates lesser energy consumption where electric demand exists.

In order to achieve increased efficiency in PV system, it is important to match the PV generators with the load impedance optimally, such that the consistency is maintained during inclement weather thus obtaining maximum power generation. Such a technique to achieve maximum power while maintaining system stability is called Maximum Power Point Tracking (MPPT). To operate the PV system at maximum power output for varying levels of temperature and solar insolation, the BLDC motor is connected to a PV module through an MPPT controller. Different methods to realize MPPT have been considered in PV power applications [8] [9-10].

A scheme wherein the use of a dedicated dc–dc converter for MPPT operation is avoided is proposed. This scheme has the PV array and battery connected in series and is designed for application in PV-powered lighting system. However, the scheme presented has the following limitations:

1) The presence of resonant elements makes the system sensitive to parameter variation;

International Journal of Research
Available at https://edupediapublications.org/journals
p-ISSN: 2348-6848
e-ISSN: 2348-795X
Volume 03 Issue 18
December 2016

2) Permissible variation in the duty ratio of the switches is limited within a certain range; and
3) Voltage gain is quite limited. A similar approach has also been reported for application in a grid-connected scheme.
However, the aforementioned schemes have to bypass the PV array by a diode and an inductor when PV power goes to zero.
This results in overall gain reduction as the PV and battery are connected in series.
In order to address the limitations encountered, a transformer-coupled dual-input converter (TCDIC)-based stand-alone scheme is proposed in this paper. The input stage of the proposed TCDIC is realized by connecting the PV array in series with the battery, thereby facilitating the boosting capability of the converter. The output voltage level of the TCDIC is further enhanced by incorporating a high-frequency step-up transformer. The unique feature of TCDIC is that it can be made to perform MPPT operation, battery charge control, and voltage boosting by employing a proper control algorithm [11-12].
Hence, all of the facilities that are achieved in the existing stand-alone schemes by involving two or more stages of dc–dc converters can be obtained by employing the proposed single stage TCDIC. A standard full-bridge inverter is employed at the output of TCDIC to achieve dc–ac conversion. The basic philosophy of this scheme and its very preliminary study have been presented, and subsequently, further work that has been carried out on this scheme is presented in this paper [13].

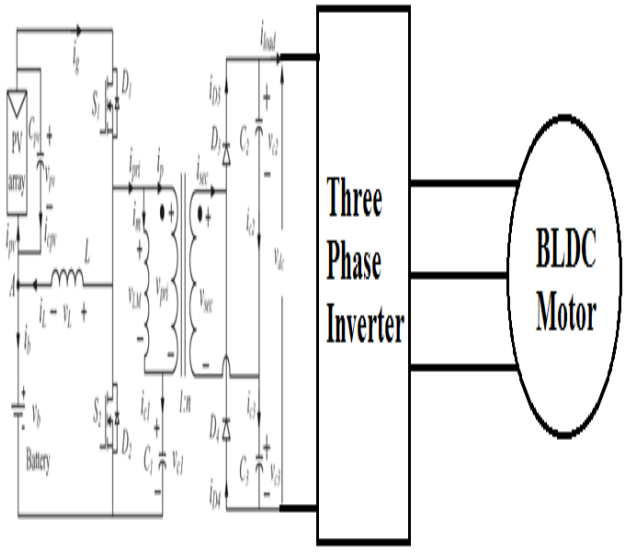

Fig. 1. Schematic circuit diagram of TCDIC for DC-AC Converter fed BLDC Drive.

II. OPERATING PRINCIPLE OF TCDIC

The schematic diagram of the TCDIC is depicted in Fig. 2. From this figure, it can be noted that no dedicated converter

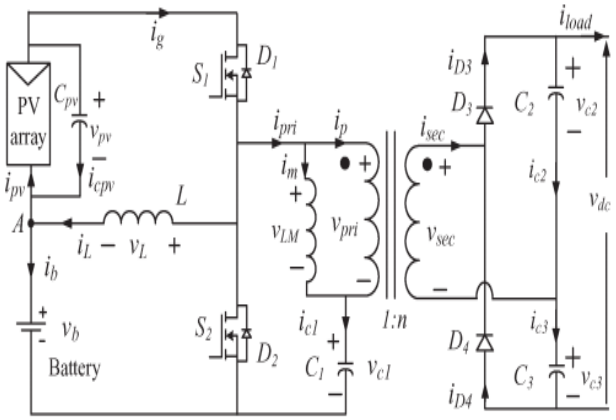

Fig. 2. Schematic circuit diagram of TCDIC.

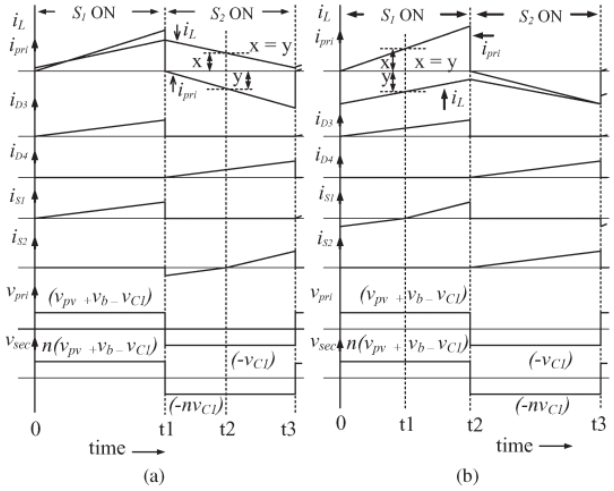

Fig. 3. Waveforms of currents flowing through and voltage across different key circuit elements of TCDIC when (a) iL is positive and (b) iL is negative.

is employed for ensuring the MPP operation of the PV array, which leads to the improved utilization of the converters involved. Furthermore, only one converter stage is present in the path between the PV array and the battery, thereby improving the charging efficiency of the battery. The inductor current iL is designed to be continuous. The switches S1 and S2 are operated in complementary fashion. All semiconductor devices and passive elements are assumed to be ideal in the following analysis.

A. Operation of the Converter When Inductor Current is Positive

The waveforms of the currents flowing through and voltages across different key circuit elements of TCDIC, while the current flowing through the inductor L is positive, are shown in Fig. 3(a). The various possible switching modes during this condition are analyzed in this section.

a) Mode I (0 to t1; S1 and D3 conducting): When S1 is turned on, the PV array voltage vpv is impressed across L, and the inductor current iL increases. During this period, the voltage impressed across the primary winding of the transformer is vpri = (vpv + vb − vC1), wherein vb is the battery voltage and vC1 is the voltage across the capacitor

International Journal of Research
Available at https://edupediapublications.org/journals
p-ISSN: 2348-6848
e-ISSN: 2348-795X
Volume 03 Issue 18
December 2016

C1. Hence, the primary current of the transformer, ipri, increases, and the capacitor C1 gets charged. The current flowing through the secondary

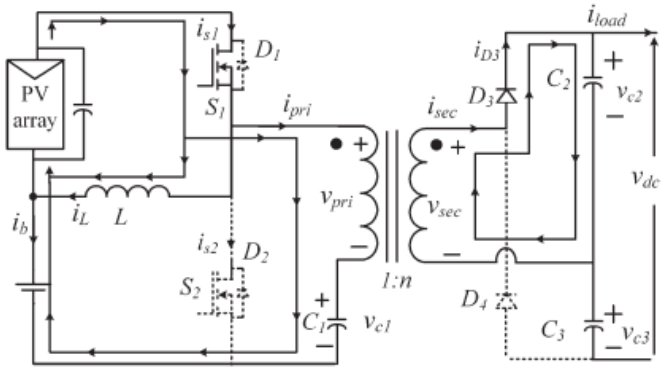

Fig. 4. Equivalent circuit diagram of TCDIC when operating in mode I and inductor current is positive.

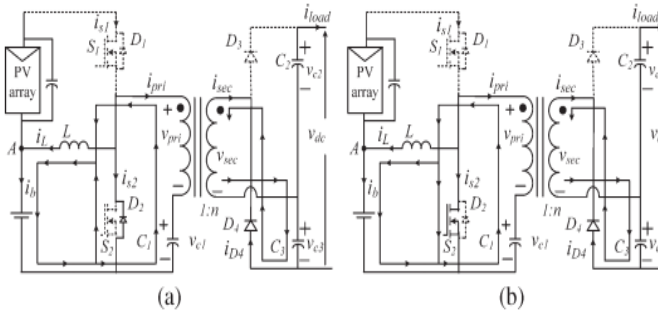

Fig. 5. Equivalent circuit diagram of TCDIC when inductor current is positive: (a) Mode II and (b) mode III.

Winding of the transformer, isec, also increases. The diode D3 is forward biased, and the capacitor C2 gets charged. The voltage across C2 is given by vC2 = n(vpv + vb − vC1), wherein n is the turns ratio of the transformer. The equivalent diagram of TCDIC during this mode is shown in Fig.4.

b) Mode II (t1 to t2; D2 and D4 conducting): This mode begins when S1 is turned off and S2 is turned on. At the starting of this mode, iL is positive, and as S1 is turned off, ipri is zero. Since iL > ipri, the diode D2 starts conducting.

The voltage impressed across L is vL = −vb, and hence, iL starts decreasing. The voltage impressed across the primary winding of the transformer is vpri = −vC1, and hence, ipri becomes negative and starts decreasing, thereby discharging C1. The current flowing through the secondary winding of the transformer, isec, reverses, and the diode D4 gets turned on. The capacitor C3 is getting charged, and the voltage across C3 can be expressed as vC3 = n(vC1). During this mode, iL > (−ipri) and diode D2 is forward biased. This mode continues until iL becomes equal to (−ipri). The equivalent circuit diagram of TCDIC during this mode is shown in Fig. 5(a).

c) Mode III (t2 to t3; S2 and D4 conducting): When iL becomes smaller than (−ipri), the diode D2 is reverse biased, and the switch S2 starts conducting. The rest of the operation remains the same as that of mode II. The equivalent circuit diagram of TCDIC during this mode is shown in Fig. 5(b).

B. Operation of the Converter When Inductor Current is Negative

The waveforms of the currents flowing through and voltages across different key circuit elements of TCDIC, while the current flowing through the inductor L is negative, are shown in Fig. 5(b). The various possible switching modes during thiscondition are analyzed in this section.

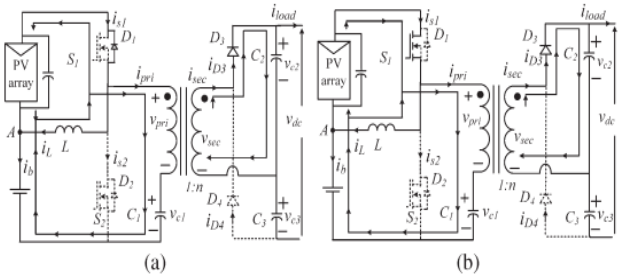

Fig. 6. Equivalent circuit diagram of TCDIC when inductor current is negative: (a) Mode I and (b) mode II.

d) Mode I (0 to t1; D1 and D3 conducting): This mode begins when S1 is turned on and S2 is turned off. At the starting of this mode, iL is negative, and ipri is zero. Hence, the diode D1 starts conducting. The rest of the operation is the same as that of mode I discussed in the previous section. This mode continues until ipri becomes equal to (−iL). The equivalent circuit diagram of TCDIC during this mode is shown in Fig. 6(a).

e) Mode II (t1 to t2; S1 and D3 conducting): When ipri becomes greater than −iL, the diode D1 is reverse biased, and the switch S1 starts conducting. The rest of the operation is the same as that of mode I discussed in the previous section. The equivalent circuit diagram of TCDIC during this mode is shown in Fig. 6(b).

f) Mode III (t2 to t3; S2 and D4 conducting): This mode begins when S1 is turned off and S2 is turned on. During this mode, both iL and ipri are negative, and the switch S2 conducts. The negative current in the primary winding of the transformer results in negative current in the secondary winding of the transformer. Hence, the diode D4 is forward biased, and the capacitor C3 gets charged. During operation in this mode, vL = −vb, vpri = −vC1, and vC3 = nvC1. The equivalent circuit diagram of TCDIC during this mode is the same as that show1n in Fig. 5(b), except that the direction of iL is reversed. From Fig. 2, the voltage vL across the inductor L can be expressed as

$$v_L = v_{pv}, \quad \text{when } S_1 \text{ is on}$$
$$v_L = -v_b, \quad \text{when } S_2 \text{ is on} \qquad (1)$$

Therefore, the average voltage drop across the inductor is

$$V_L = DV_{pv} - (1-D)V_b$$

Wherein D is the duty ratio of the switch S1. Equating the average voltage drop across the inductor to zero,

International Journal of Research
Available at https://edupediapublications.org/journals
p-ISSN: 2348-6848
e-ISSN: 2348-795X
Volume 03 Issue 18
December 2016

$$V_{pv} = \left[\frac{(1-D)}{D}\right] V_b \quad (2)$$

From (2), it can be inferred that the PV voltage can be controlled by manipulating D as battery voltage Vb can be assumed to be a stiff source. Therefore, the MPPT operation of the PV array can be achieved through a proper manipulation of D. The average output voltage of the TCDIC, Vdc, is given by

$$\begin{aligned} V_{dc} &= (V_{C_2} + V_{C_3}) \\ &= [n(V_b + V_{pv} - V_{C_1}) + nV_{C_1}] \\ &= n(V_b + V_{pv}). \end{aligned} \quad (3)$$

Applying KCL at point A of Fig. 2,

$$i_L + i_{cpv} = i_b + i_{pv} \quad (4)$$

Considering the average values of iL, icpv, ib, and ipv over a switching cycle and noting that $\bar{}$ icpv = 0, (4) transforms to

$$I_b = I_L - I_{pv} \quad (5)$$

From (5), it can be noted that, for IL > Ipv, the battery is charged and, for IL < Ipv, the battery is discharged. Therefore, by controlling IL, for a given Ipv, battery charging and discharging can be controlled. The drawback of TCDIC and the associated design constraints are presented. The details of the control strategy devised for TCDIC are discussed.

III. CONTROL STRUCTURE

The controller of a stand-alone system is required to perform the following tasks: 1) extraction of maximum power from the PV array; 2) manipulate the battery usage without violating the limits of overcharge and over discharge; and 3) dc–ac conversion while maintaining the load voltage at the prescribed level. A controller is devised for manipulating the TCDIC to realize the first two aforementioned objectives, while the third objective is achieved by employing a conventional proportional integral (PI) controller to control the output voltage of the full bridge inverter through sinusoidal pulse width modulation. As the conventional control scheme is used for controlling the output voltage of the inverter, its design issues are not discussed in this paper. The details of the control algorithm devised for TCDIC are presented in this section. In order to achieve the desired functionalities, TCDIC is required to operate in one of the following modes.

1) MPPT mode: Maximum power is extracted from the PV array when the system is operating in this mode. However, in order to operate in this mode, one of the following conditions must be satisfied: 1) Available maximum PV power Pmpp is more than the load demand Pl, and the surplus power can be consumed by the battery without being overcharged; and 2) Pmpp < Pl and the battery have the capability to supply Pl − Pmpp without being overdischarged. The PV power in MPPT mode is given by Ppv = Pmpp = (Pb + Pl), where Pb is the battery power which is defined as positive during charging and negative while discharging.

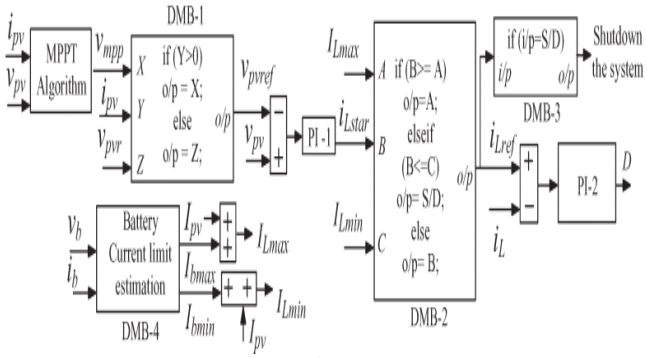

Fig. 7. Control structure for the proposed TCDIC.

2) Non-MPPT mode: Based on the state of charge (SOC) level of the battery, its charging current is required to be limited to a maximum permissible limit Ib max to prevent the battery from getting damaged due to overcharge. The maximum charging current limit Ib max restricts the maximum power that can be absorbed by the battery to Pb max = Ib max ∗ Vb. When Pmpp > Pl and the surplus power is more than Pb max, the system cannot be operated in MPPT mode as it would overcharge the battery. During this condition, power extraction from PV is reduced to a value given by Ppv = (Pb max + Pl). This mode of operation is known as non-MPPT mode.

3) Battery only (BO) mode: The system operates in BO mode when there is no PV power and the battery has the capability to supply the load demand without being over discharged.

4) Shutdown mode: When Pmpp < Pl and the battery does not have the capability to supply Pl − Pmpp, the system needs to be shut down to prevent the battery from being over discharged.

The control algorithm that is employed to select the proper mode of operation for the TCDIC, depending on the status of the SOC of the battery vis-a-vis the availability of power from the solar array, is shown in Fig.8. The proper mode selection is done by four logical decision-making blocks (DMBs). The control block DMB-1 sets the reference for the PV array voltage (Vpvref). It also decides whether the system will operate in BO mode or in MPPT mode. When it is found that ipv > 0, thereby indicating the availability of PV power, the MPPT mode of operation is selected, and the output of the MPPT algorithm block (i.e., Vmpp) sets Vpvref . When the PV power is not available, the BO mode is selected, and Vpvref is taken as Vpvr wherein Vpvr is selected so as to maintain the output voltage Vdc within the desired range of 350–460 V as per (3). The error between Vpvref and VP V is passed through a PI controller to set the required reference for the inductor current (iLstar). An upper limit IL max and a lower limit IL min is imposed on iLstar based on the relationship given in (5) to prevent

International Journal of Research
Available at https://edupediapublications.org/journals
p-ISSN: 2348-6848
e-ISSN: 2348-795X
Volume 03 Issue 18
December 2016

overcharging and overdischarging of the battery, respectively. These two limits are derived as follows:

$$I_{L\max} = I_{b\max} + I_{pv}$$
$$I_{L\min} = I_{b\min} + I_{pv}$$

Wherein Ib max and Ib min are the maximum permissible charging and discharging current of the battery, respectively. These two limits are set based on the SOC level and the allowable depth of discharge of the battery. The block DMB-4 is employed to carry out the aforementioned functions. The block DMB-2 sets the reference level for the inductor current iLref after resolving the constraints imposed by IL max and IL min.

When iLref remains within its prescribed limit, the system operates either in MPPT mode (for ipv > 0) or in BO mode (for ipv ≤ 0). When iLref hits its lower limit, thereby indicating that the overdischarge limit of the battery is reached, DMB-3 withdraws gating pulses from all the switches and shuts down the system. When the battery overcharging limit is attained,iLref hits its upper limit. This situation arises only when thesystem is operating in MPPT mode with Pmpp > Pl and thesurplus power is more than Pb max. In this condition, iLref is limited to IL max to limit the battery charging current to Ib max, and the MPPT is bypassed. As the battery charging current is limited to Ib max, power consumed by the battery is restricted to Pb max. This makes the available PV power more than (Pl + Pb max). This extra PV power starts charging the PV capacitor, and its voltage increases beyond Vmpp, thereby shifting the PV operating point toward the right side of the MPP point, and the power extracted from the PV array reduces. This process continues until the power drawn from the PV array becomes equal to (Pl + Pb max). Hence, during operation of the system in nonMPPT mode, the PV array is operated at a point on the right side of its true MPP, and hence, Ppv < Pmpp. If there is a decrement in load demand while operating in non-MPPT mode, power drawn from the PV array becomes more than (Pl + Pb max), and this excess power drawn starts charging the PV capacitor, thereby shifting the operating point of the PV further toward the right side of its previous operating point. In case of an increment in the load demand, the power drawn from the PV array falls short of supplying the load demand and the dc-link capacitors, and the PV capacitor starts discharging. As the voltage of the PV capacitor falls, the operating point of the PV array shifts toward the left side from its previous operating point. This leads to an increment in the power drawn from the PV array, and this process continues until the power balance is restored. In case the load demand increases to an extent such that the PV power available at its MPP falls short to supply this load, the battery will come out of its charging mode, iLref will become less than IL max, and the system operates in MPPT mode.

IV. BLDC MOTOR

The brush less dc engine comprise of four fundamental parts Power converter, changeless magnet brushless DC Motor (BLDCM), sensors and control calculation. The force converter changes power from the source to the BLDCM which thus changes over electrical vitality to mechanical vitality. One of the remarkable highlights of the brush less dc engine is the rotor position sensors, in view of the rotor position and order signals which may be a torque charge, voltage summon, rate order etc; the control calculation s focus the entryway sign to every semiconductor in the force electronic converter.

The structure of the control calculations decides the sort of the brush less dc engine of which there are two principle classes voltage source based drives and current source based drives. Both voltage source and current source based commute utilized for perpetual magnet brushless DC machine. Be that as it may, machine with a non sinusoidal back emf brings about diminishment in the inverter size and lessens misfortunes for the same influence level.

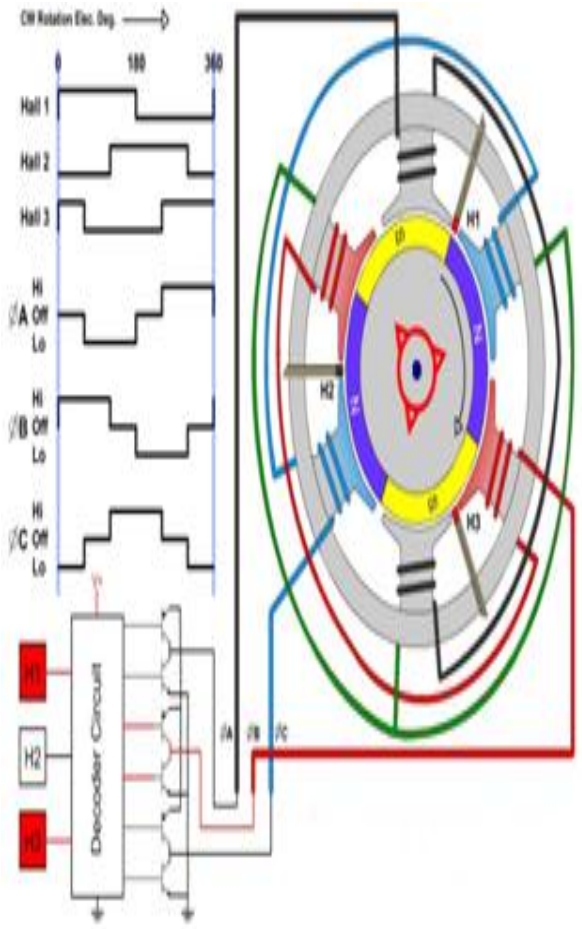

International Journal of Research
Available at https://edupediapublications.org/journals
p-ISSN: 2348-6848
e-ISSN: 2348-795X
Volume 03 Issue 18
December 2016

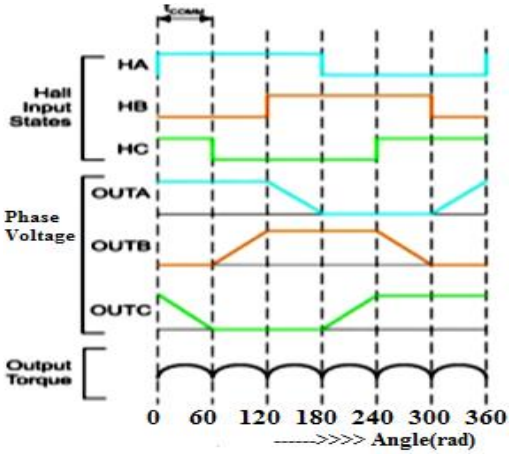

Fig.8.Four-Pole Brushless motor, Hall signals & Stator voltages Commutation, drive and winding timings.

V.MATLAB/SIMULATION RESULTS

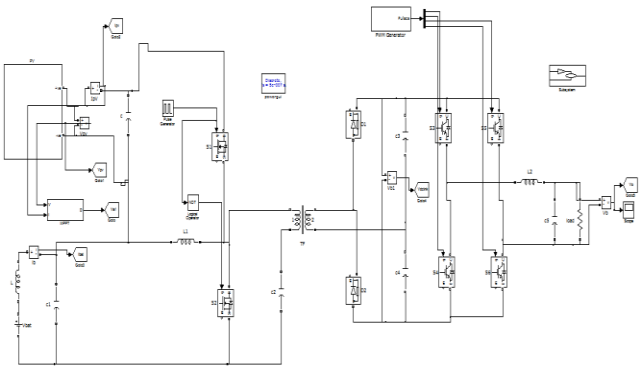

Fig.9.Matlab/Simulation model of under steady-state operation.

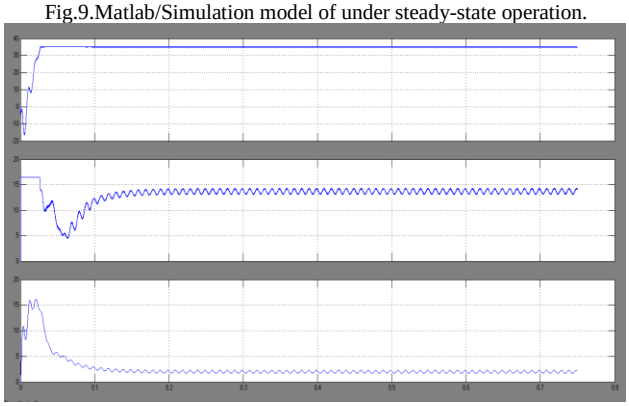

(a)

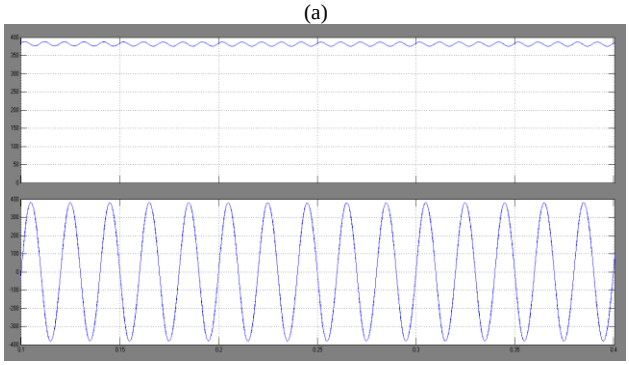

(b)

Fig. 10. Simulated response of the system under steady-state operation in MPPT mode. (a) vpv, ipv, and ib. (b) vdc and load voltage.

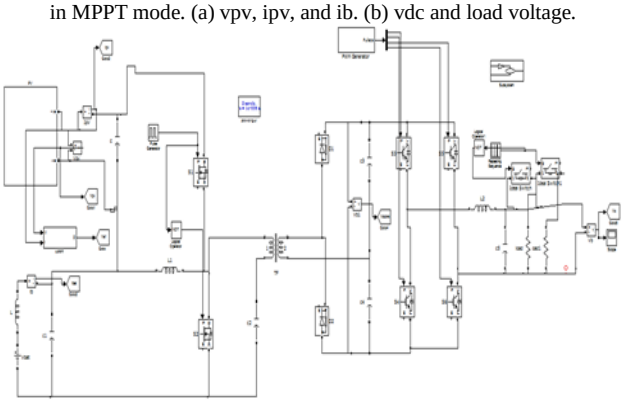

Fig.11. Matlab/Simulation model of under changes in load and insolation level while operating in MPPT mode.

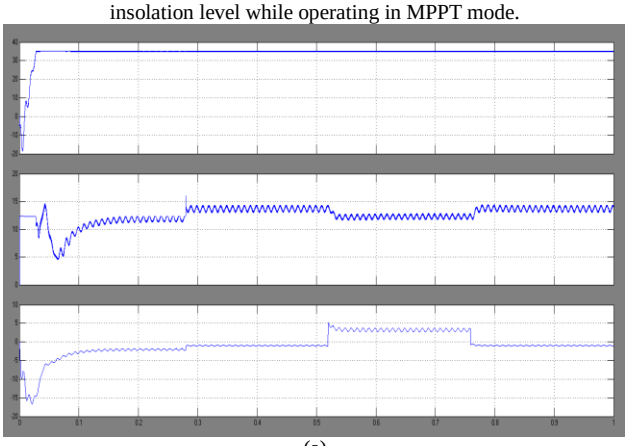

(a)

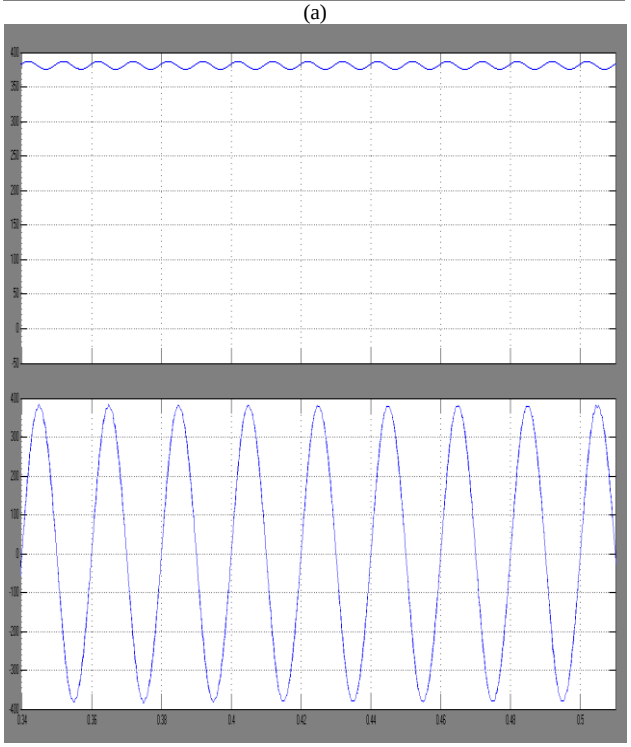

(b)

Fig. 12. Simulated response of the system under changes in load and insolation level while operating in MPPT mode. (a) vpv, ipv, and ib. (b) vdc and load voltage.

International Journal of Research
Available at https://edupediapublications.org/journals
p-ISSN: 2348-6848
e-ISSN: 2348-795X
Volume 03 Issue 18
December 2016

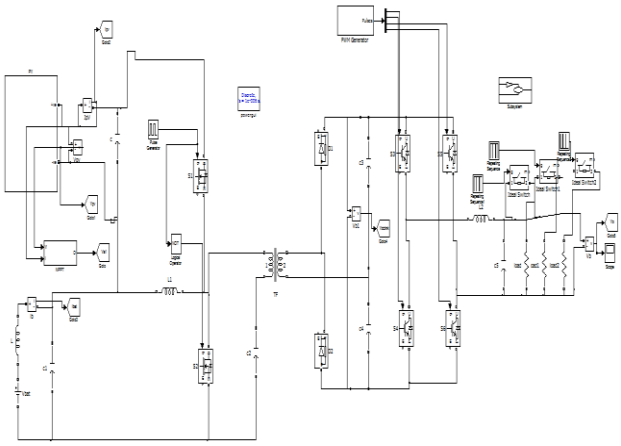

Fig.13. Matlab/Simulation model of under mode transition between MPPT and non MPPT mode and the effect of load change in non-MPPT mode.

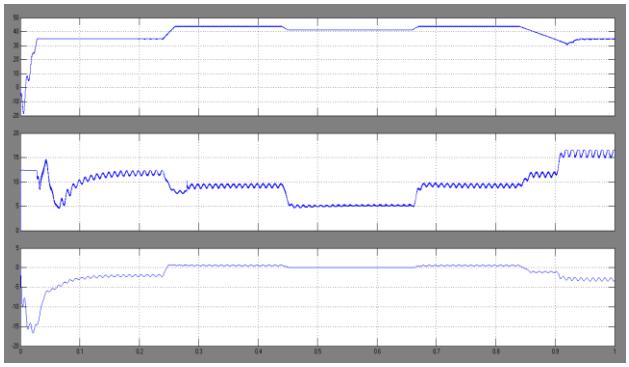

(a)

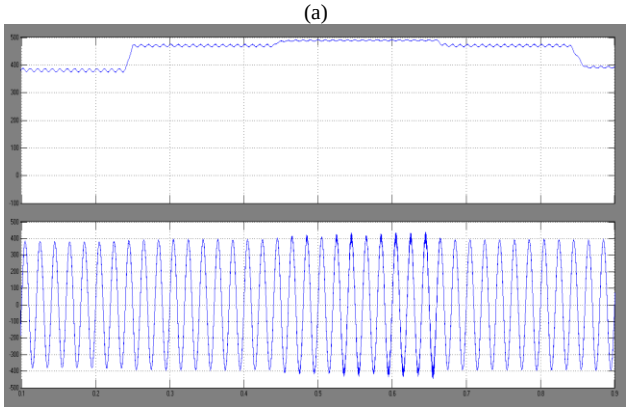

(b)

Fig. 14. Simulated response of the system under mode transition between MPPT and non-MPPT mode and the effect of load change in non-MPPT mode. (a) vpv, ipv, and ib. (b) vdc and load voltage.

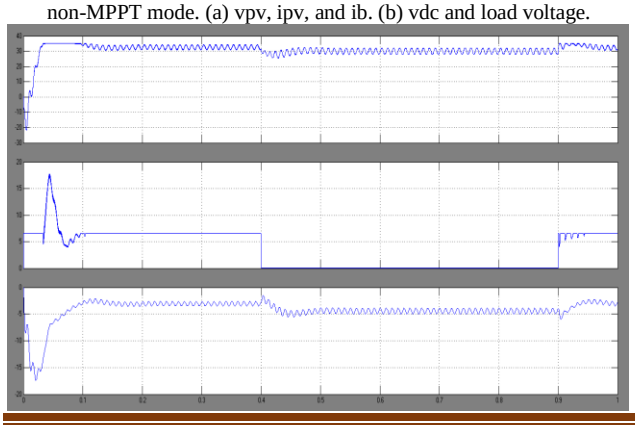

(a)

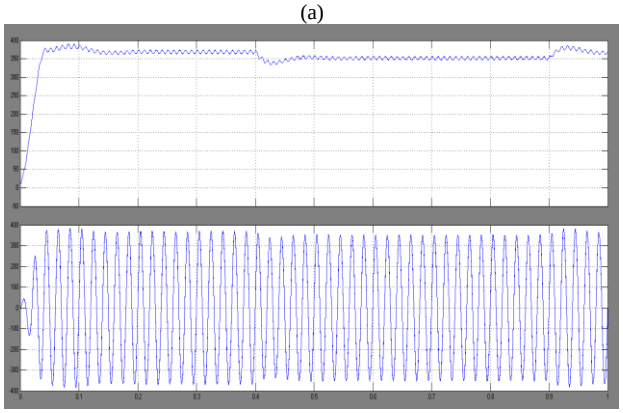

(b)

Fig. 15. Response of the simulated system during mode transition between MPPT and BO modes. (a) vpv, ipv, and ib. (b) vdc and load voltage.

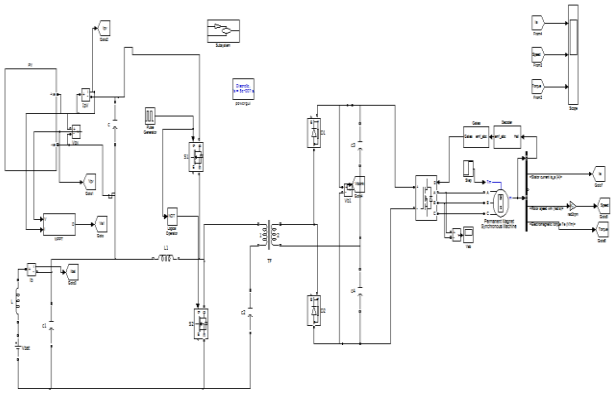

Fig.16.Matlab/Simulation model of the three phase inverter fed BLDC Drive.

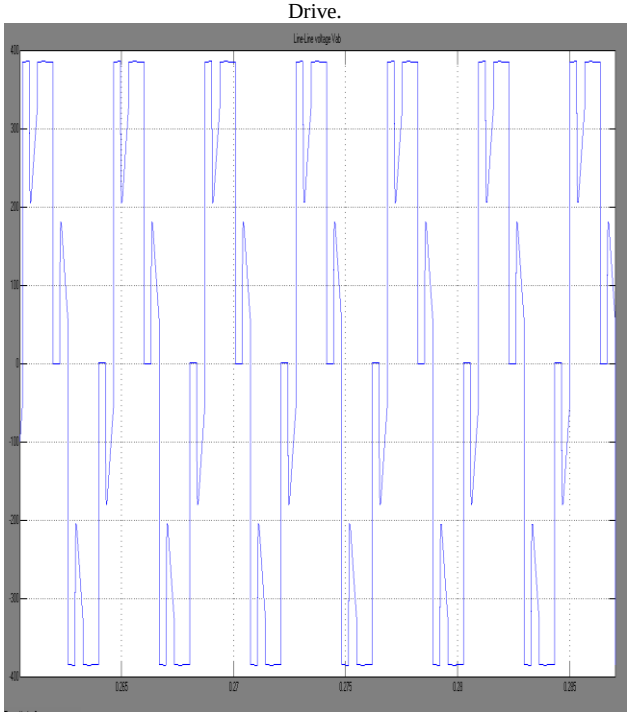

Fig.17.Inverter line to line Voltage.

International Journal of Research
Available at https://edupediapublications.org/journals
p-ISSN: 2348-6848
e-ISSN: 2348-795X
Volume 03 Issue 18
December 2016

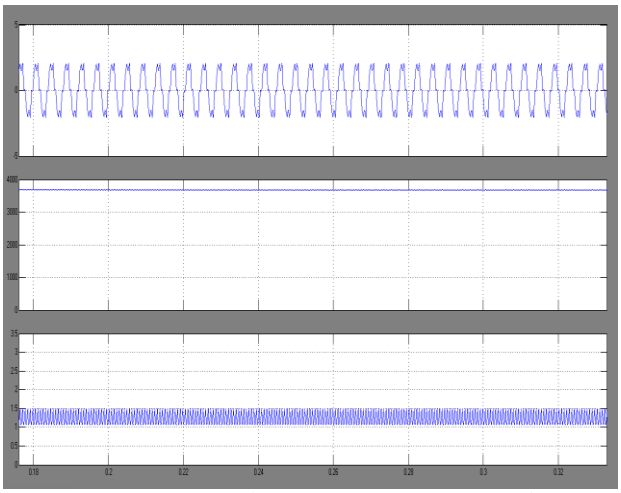

Fig.18.Simulation results forstator current,speed, torque, of BLDC motor.

VI.CONCLUSION

A solar PV-based stand-alone scheme for application in rural areas is proposed in this paper. It is realized by involving a new TCDIC followed by a conventional full-bridge dc to ac inverter. Performances of the management in real conditions strongly depend of the accuracy of the forecasts and of the mode of operation. This important conclusion leads to many questions about reactive power management without denying the importance and the necessity of the predictive optimization stage. A suitable control strategy for the proposed TCDIC devised for manipulating the TCDIC to realize the first two aforementioned objectives, while the third objective is achieved by employing a conventional proportional integral (PI) controller to control the output voltage of the full bridge inverter through sinusoidal pulse width modulation. Due to significant increase in the demand of electric motors, design and manufacturing of high efficiency motors and related variable speed drives has been a major interest by many suppliers. Brushless DC (BLDC) motor has many advantages including high torque capability. In this context, next and future works will deal with reactive management for real condition operations.

REFERENCES

[1]. Hamid R. Teymour, Danny Sutanto, Kashem M. Muttaqi, and P. Ciufo, ―Solar PV and Battery Storage Integration using a New Configuration of a Three-Level NPC Inverter With Advanced Control Strategy ‖IEEE transactions on energy conversion, vol. 29, no. 2, June, 2014.

[2]. O. M. Toledo, D. O. Filho, and A. S. A. C. Diniz,―Distributed photovoltaic generation and energy storage systems: A review,‖ Renewable Sustainable Energy, Rev., vol. 14, no. 1, pp. 506–511, 2010.

[3]. M. Bragard, N. Soltau, S. Thomas, and R. W. De Doncker, ―The balance of renewable sources and userdemands in grids: Power electronics for modular battery energy storage systems,‖ IEEE Trans. Power Electron., vol. 25, no. 12, pp. 3049–3056, Dec. 2010.

[4]. Muhammad H. Rashid, ―Power electronics circuits, devices and applications‖ Pearson education, 3rdedition, 2004.

[5]. Lewicki, Z. Krzeminski, and H. Abu-Rub, ―Spacevector pulse width modulation for three-level npc converter with the neutral point voltage control,‖ IEEE Trans. Ind. Electron., vol. 58, no. 11, pp. 5076–5086, Nov., 2011.

[6] M. Miyatake, M. Veerachary, F. Toriumi, N. Fujii, and H. Ko, "Maximum power point tracking of multiple photovoltaic arrays: A PSO approach," IEEE Trans. Aerosp. Electron. Syst., vol. 47, no. 1, pp. 367 380, Jan. 2011.

[7] J. T. Stauth, M. D. Seeman, and K. Kesarwani, "Resonant switched capacitor converters for sub-module distributed photovoltaic power management," IEEE Trans. Power Electron., vol. 28, no. 3, pp. 1189–1198, Mar. 2013.

[8] T. Shimizu, M. Hirakata, T. Kamezawa, and H. Watanabe, "Generation control circuit for photovoltaic modules," IEEE Trans. Power Electron., vol. 16, no. 3, pp. 293–300, May 2001.

[9] H. J. Bergveld et al., "Module-level dc/dc conversion for photovoltaic systems: The delta-conversion concept," IEEE Trans. Power Electron., vol. 28, no. 4, pp. 2005–2013, Apr. 2013.

[10] P. S. Shenoy, K. A. Kim, B. B. Johnson, and P. T. Krein, "Differential power processing for increased energy production and reliability of photovoltaic systems," IEEE Trans. Power Electron., vol. 28, no. 6, pp. 2968–2979, Jun. 2013.

[11] J. H. Wohlgemuth and S. R. Kurtz, "How can we make PV modules safer?" in Proc. 38th IEEE Photovoltaic Spec. Conf., 2012, pp. 3162–3165.

[12] W. Li and X. He, "Review of non-isolated high-step-up dc/dc converters in photovoltaic grid-connected applications," IEEE Trans. Ind. Electron., vol. 58, no. 4, pp. 1239–1250, Apr. 2011.

[13] H. Wang and D. Zhang, "The stand-alone PV generation system with parallel battery charger," in Proc. IEEE ICECE, Jun. 2010, pp. 4450 4453.